Nanoscale optical features via hot-stamping of As_2Se_3 glass

Sylvain Danto[a,b], Erick Koontz[a,b], Yi Zou[c], Tony. O. Ogbuu[c], Benn Gleason[a,b], Peter Wachtel[a,b], Jonathan D. Musgraves[a,b,d], Juejun Hu[c], Kathleen Richardson[a,b]

[a]Glass Processing and Characterization Laboratory (GPCL), College of Optics and Photonics/ CREOL - University of Central Florida, Orlando FL, 32816 USA
[b]Department of Materials Science and Engineering, COMSET, Clemson University, Clemson, SC 29634
[c]Department of Materials Science & Engineering, University of Delaware, Newark, DE 19716, USA
[d]IRradiance Glass, Inc. 3564 Avalon Park Blvd E, Suite #226, Orlando, FL 32828

ABSTRACT

Here we show our ability to fabricate two-dimensional (2D) gratings on chalcogenide glasses with peak-to-valley amplitude of ~200 nm. The fabrication method relies on the thermal nano-imprinting of the glass substrate or film in direct contact with a patterned stamp. Stamping experiments are carried out using a bench-top precision glass-molding machine, both on As_2Se_3 optically-polished bulk samples and thermally-evaporated thin films. The stamps consist of silicon wafers patterned with sub-micron lithographically defined features. We demonstrate that the fabrication method described here enables precise control of the glass' viscosity, mitigates risks associated with internal structural damages such as dewetting, or parasitic crystallization. The stamping fidelity as a function of the Time-Force-Temperature regime is discussed, and further developments and potential applications are presented.

Keyword list *Chalcogenide – Glass – Hot-pressing - Nanoimprinting - Patterning*

1. INTRODUCTION

Surface nano-structuring, often referred to generally as nano-imprinting, offers endless possibilities for creating novel devices, with applications spanning photonics, microelectronics, biosensors, and surface science. Photolithography and related methods rely on a radiation source (UV, electron beam, X-ray or ions) to create a desired pattern onto a photosensitive resist material previously coated to a substrate. These methods are well-established technologies for prototyping, low-volume work and mask production but have yet to be demonstrated suitable for larger scale/area applications. Typically, these approaches require large equipment and operating investment that strongly limit their potential and make them incompatible with high-throughput roll-to-roll processing. Alternative strategies such as ink-jet [1], soft lithography [2], or reaction-diffusion [3] printing have been developed recently to increase manufacturing yield, transfer fidelity and resolution while driving complexity and cost downward. While nanoimprint lithography (NIL) [4-6] allows micrometer-scale and sub-hundred-nanometer resolution as well as 3D structure fabrication, translation to larger areas is often limited by the 'patterning' process methodology.

Traditionally the basic NIL process is based on the use of thermoplastic or cross-linkable polymers that serve as 'soft' stamps that can deform and rigidify in the mold crevices and features. In the present effort we explored direct hard-stamp nanoimprinting as a cost-effective patterning method for transferring complex nanometer-sized structures onto chalcogenide glasses (ChGs). ChGs contain group VI chalcogen species sulfur (S), selenium (Se) and/or tellurium (Te), with other group IV or V elements. These glasses have an infinitely large capacity for composition alloying with glass-formers such as As, Sb, Ge or Ga, enabling large, continuous tuning of their thermo-mechanical and optical properties. ChGs have been extensively studied due to their mid-infrared (MIR) transparency, optical non-linearity, photo-sensitivity and phase-change ability [7, 8] and within the past decade their use in bulk, planar and fiber optics has expanded considerably as their design and processing flexibility for these forms has enabled use in a range of photonic applications [9]. Furthermore ChGs offer interesting properties exploitable for the collective management of photons for photovoltaic applications. Their optical band gap energies, typically situated between 1.5 to 2.5 eV, and can be tuned to match the weak absorption wavelength regimes of a-Si, c-Si, CIGS, CdTe, and organic solar materials. Unlike crystalline

Corresponding author sdanto@g.clemson.edu

Optifab 2013, edited by Julie L. Bentley, Matthias Pfaff, Proc. of SPIE Vol. 8884, 88841T

materials that exhibit abrupt viscosity changes at the melting point when heated, ChGs feature a smooth viscosity-temperature curve, making them amenable to shaping, either in bulk, planar film or fiber form, or to solution-based processing routes for large-area coating strategies [10, 11]. In addition it allows direct structure formation in glasses. Fabrication of ChG optical components, such as waveguides and resonators, has been demonstrated by standard photolithography [12, 13], e-beam patterning [14], solution-derived method [15] or hot nanoimprint [16, 17].

Taking full advantage of these attractive attributes, we explored the feasibility of fabricating 2D symmetric and asymmetric gratings on ChGs with nanoscale peak-to-valley amplitude. Based on its known thermal stability against crystallization, we have selected for these experiments the canonical stoichiometric As_2Se_3 compound (also referred to as $As_{40}Se_{60}$, based on its relative mol fractional constituent level). Efforts to impose surface structure on the bulk forms of this composition were carried out and then extended to thermally evaporated glass films. Here, the bulk glass or deposited glass film is brought in contact with a patterned silicon wafer and held above its glass transition temperature (T_g) for a certain time-temperature regime under an applied load, so that the glass flow conforms to the shape of the stamp pattern. A range of process parameters has been progressively refined leading towards conditions that yield good transfer fidelity and post-stamped surface quality. The stamping fidelity is discussed and further developments are presented.

2. METHOD

Nanoimprint experiments were carried out on bulk glass and thermally evaporated thin films using a research grade precision glass-molding machine manufactured by Dyna Technologies Inc. (DTI's GP-5000HT press). It is a bench-top molding machine with the precision of a standalone-molding machine, which also possesses the flexibility, functionality and control over process parameters needed for research and laboratory testing (Fig. 1a). Attributes of the system are discussed elsewhere [18].

The proposed single-step imprint process starts with the fabrication of the glass sample and stamps. The synthesis of the bulk glass As_2Se_3 was carried out by the co-fusion of the raw elements under vacuum in quartz reaction tubes. The melt is rocked overnight above T_m to ensure melt homogeneity and then rapidly quenched in air. All syntheses were carried out using high-purity starting reagents (As: Alfa Aesar 5N, Se: Alfa Aesar 5N). In order to investigate stamping fidelity, we have carried out tests on the glass in bulk and in thin film forms (Fig. 1b). In the first case the glass rod is cut into a disk of 10 mm diameter and 2 mm thickness with both faces parallels and optically polished. In the second case powdered glass is deposited by thermal evaporation in a ~2.15 µm-thick layer; the deposition substrate consist of 3" silicon wafers coated with 3 µm thick thermal SiO_2. Uniform thickness films with dense micro-structures free of defects are obtained in this manner. Stamps are fabricated through gray-scale lithography to etch silicon wafers with a KOH solution to engrave parallel grooves of various widths and heights.

For each test, the glass film and stamp are inserted in the DTI press and subjected to a Force-Temperature-Time profile schematically depicted in Fig. 1c. The first stage, or heating stage, involves heating the glass sample at the temperature of stamping (1. $T_{stamping}$), with $T_{stamping}$ higher than the glass transition temperature of the glass ($T_{g\ As2Se3}$ = 190 °C), so that it becomes less viscous. Heating rates during this stage range from 50-75 °C per minute. During the second stage (soaking), the glass sample is held at a constant force (2. $F_{soaking}$) for a set time (3. $t_{soaking}$), and allowed to thermally equilibrate. The third stage involves applying a pressing force (4. $F_{stamping}$) to the glass sample for a few minutes (5. $t_{stamping}$), which conforms the sample to the shape of the adjacent mold surfaces. It is assumed at this stage that the glass is fluid enough at the equilibrating 'soak' temperature that the applied load causes the material to flow and conform to the shape of the stamp pattern. Optimum press conditions required to define conditions of glass flow are guided by prior knowledge of the base glass' viscosity temperature behavior [19]. The final stage is the cooling stage, in which the sample is brought back to room temperature.

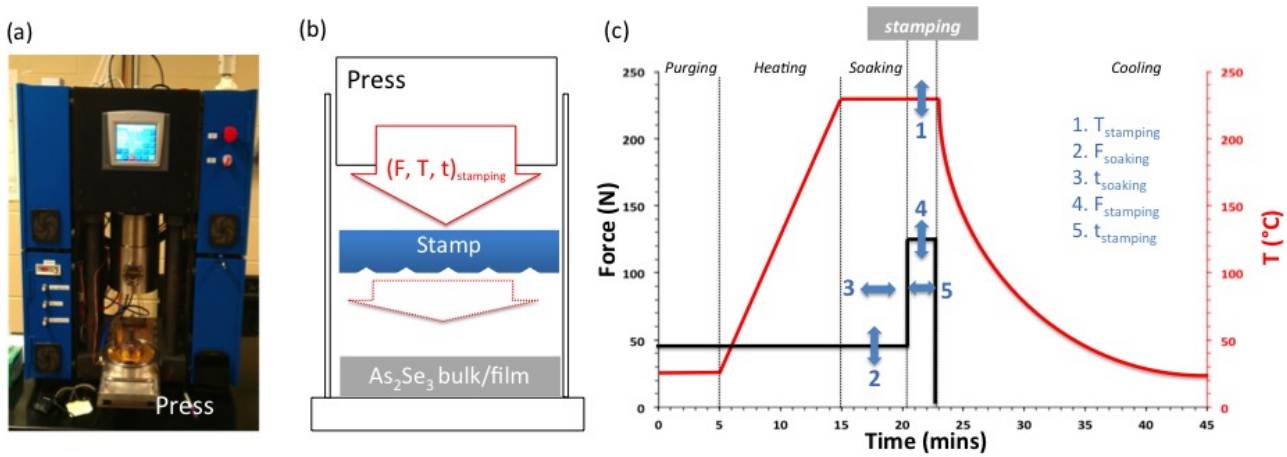

Fig. 1. Hot-stamping on As_2Se_3 glass **(a)** DTI press **(b)** schematic representation of the experiment **(c)** Force-Temperature-Time profile

Post-stamping, the glass surface is inspected to evaluate surface quality and stamping fidelity. The surfaces of the glass film and stamp are optically interrogated to estimate the glass area impacted by the stamping, and to detect evidence of incomplete stamp/surface contact and/or possible dewetting. Non-contact white light interferometric microscopy (Zygo Corp. model NewView 6300) is used to assess large-scale roughness measurement and estimation of film thickness uniformity. In order to assess imprinted feature's peak height and width, stamped bulk samples were examined using scanning electron microscope (SEM; Hitachi model S3400 SEM). Each sample was coated with a thin conductive platinum layer (~500 nm) to enable viewing.

3. RESULTS AND DISCUSSION

The stamping of the As_2Se_3 glass bulk is schematically depicted in Fig. 2a. The stamp consists of a silicon wafer (~8x8mm^2) engraved with parallel grooves of 2.50 µm in depth and of groove widths spanning 5, 7, 10, 15, 20 and 30 µm. Depicted in Fig. 2b is the SEM micrograph of the stamped sample (process parameters: $F_{soaking}$ = 0 lbs (0 N), $t_{soaking}$ = 5 mins, $T_{stamping}$ = 210 °C, $F_{stamping}$ = 25 lbs (111 N), $t_{stamping}$ = 3 mins). No evidence of crystallization at the surface of the glass is observed after nanoimprinting. When compared with pre-stamping surface topology (panel (a)), the SEM micrograph on Fig. 3b reveals that the stamping process allows the wafer's features to be transferred onto the whole surface of the glass.

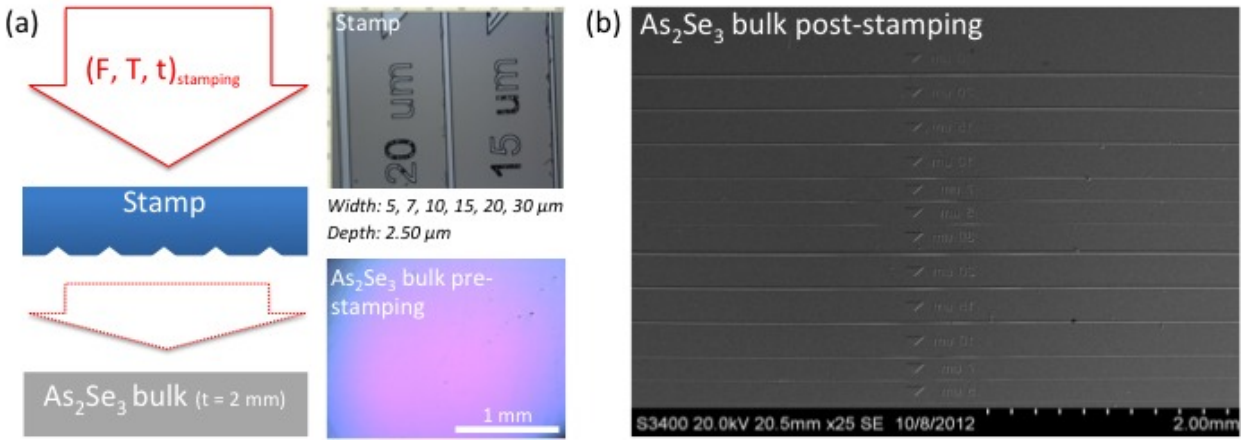

Fig. 2. NIL on As_2Se_3 bulk glass (2-mm thick, 10-mm diameter) **(a)** Scheme of the experiment; optical micrographs of the stamp (grooves width: 5, 7, 10, 15, 20, 30 µm, depth: 2.50 µm) and of the glass before stamping **(b)** SEM micrograph of the glass post-stamping.

Result of interferometric microscopy is shown on Fig. 3. As illustrated in Fig. 3a, the dimension of the glass features is in good agreement with the dimension of the largest grooves (height ~2.50 µm and width ~20 and 30 µm). The peak-to-valley profile across a diagonal line (Fig. 3b) shows good consistency of the peak height at 2.50 µm. However we note that the transfer of the thinner grooves (5 and 7 µm) is incomplete. The explanation of this result remains, to this date, speculative but we assume that the glass fluidity is not sufficiently high at the equilibrating 'soak' temperature to cause the material to flow and conform to the shape of the stamp pattern. Alternatively, or in conjunction, we believe it can be due to post-stamping thermal and/or mechanical shocks weakening the thin stretches of glass.

We have demonstrated here our ability to imprint straight lines with a dimension of several microns wide and 2.5 microns high on As_2Se_3 bulk material. Yet thin film configuration with gratings having dimension in sub-micron scale might be more suitable for device integration such as solar cells. Following experiments on bulk samples, we have conducted hard stamping test on As_2Se_3 glass thin films. The scheme of the experiment and process parameters are shown in Fig. 3. The stamp is made of a silicon wafer (~8x8mm^2) engraved with parallel grooves of ~0.20 µm in depth and width (Fig. 3a).

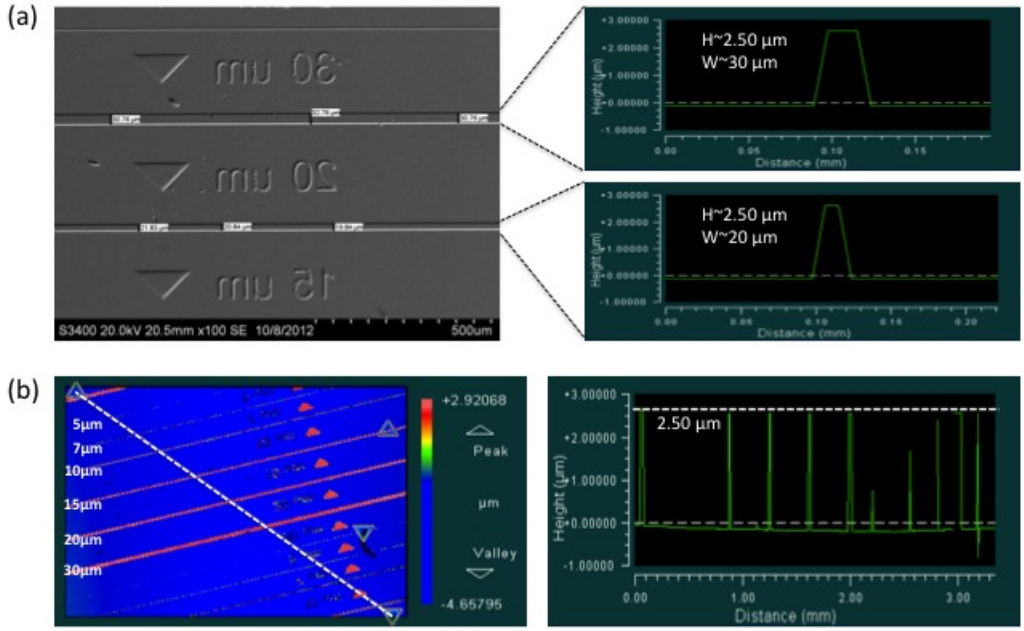

Fig. 3. NIL on As_2Se_3 bulk glass **(a)** SEM micrograph and peak-to-valley profile of 20 and 30 µm grooves **(b)** Top-view and peak-to-valley profile across one specific line

Summarized in Fig. 3b the process parameters and experimental outputs for four samples (noted 'a' to 'd' respectively). The soaking force and time are set at 0 lbs and 5 minutes respectively, and the stamping temperature at 235 °C. The stamping force $F_{stamping}$ ranges 20 to 30 lbs (89 to 133 N) and the stamping time 1.5 or 2 mins. Very low-quality transfer fidelity is achieved for samples 'a', 'c' and 'd'; dewetted patches are observed on these samples and the glassy features reache only a fraction of the groove's depth.

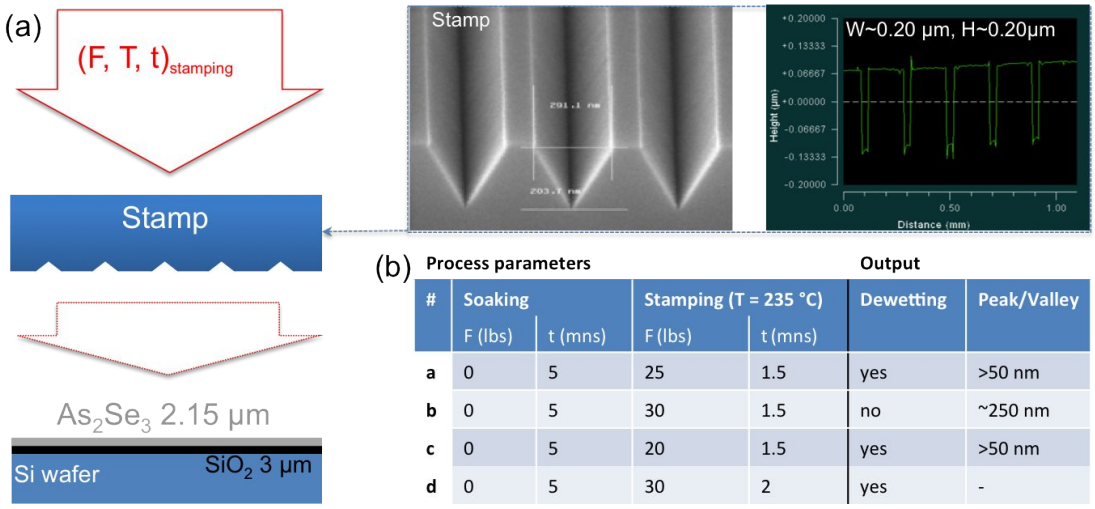

(b)

#	Process parameters: Soaking F (lbs)	Soaking t (mns)	Stamping (T = 235 °C) F (lbs)	Stamping (T = 235 °C) t (mns)	Output: Dewetting	Output: Peak/Valley
a	0	5	25	1.5	yes	>50 nm
b	0	5	30	1.5	no	~250 nm
c	0	5	20	1.5	yes	>50 nm
d	0	5	30	2	yes	-

Fig. 4. NIL on As_2Se_3 thin film (2.15 µm in thickness) **(a)** Scheme of the experiment; SEM micrograph of V-grooves etched on Si wafers using KOH and peak-to-valley profile (V-grooves depth and width 0.20 µm) **(b)** Process parameters and stamping output for four samples

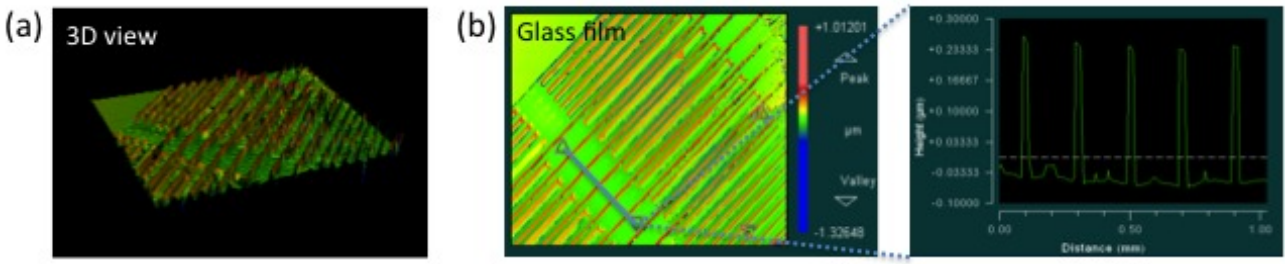

Fig. 5. NIL on As_2Se_3 thin film **(a)** 3D view **(b)** top-view and peak-to-valley profile across one specific line

Best transfer is obtained for the sample 'b' (Fig. 5) with F_{mold} = 30 lbs (139 N), t_{stamp} = 1.5 mins. As can be seen no evidence of dewetting is observed. The height of the glass features, ~250 nm, is in relatively good agreement with the expected groove depths (~200 nm) at the surface of the Si wafer. Furthermore the peak-to-valley values of the glassy features are very homogenous across the film.

We have aimed at unraveling how process parameters used during the stamping cycle impact the final, post-pressed quality of an As_2Se_3 glass surface. Further developments are in progress to mitigate risks associated with nanoimprint development, such as issues with integrity of the shape, dewetting, crossed-contamination or parasitic crystallization. The basic NIL process is based on the physical deformation of a thermo-viscous material under applied pressure and at elevated temperatures. The processing temperature we used for imprinting As_2Se_3 glass is 210 °C in bulk form and 235 °C in thin film form; this difference is due to the strong adhesion of the glass on the silica wafer, which necessitates an increase in the stamping temperature. Temperatures at this point remained suitably high to enable flow, without approaching the temperature at which glass volatilization takes place. Yet, as part of the drive to understand the effect of pressing parameters on feature transfer and to reduce the overall energy-time stamping budget, it will be of interest for future process development to reduce the viscosity of the grating glass material. Already, preliminary soft stamp experiments on the $As_{20}Se_{80}$ glass (T_g = 109 °C) show that this composition can be pressed at temperatures in the 100-140°C range. Lower fabrication and processing temperatures along with a marked decrease in dimensionality and connectivity in the glass network should result in a glass that is "easier" to press.

Though glass thermal properties may vary, it is reasonable to expect that the same areas will prove similarly challenging in all cases. A non-trivial consideration not largely examined in this initial part of our study relates to the fact that despite being compositionally identical to the parent bulk glass material, it is well known from prior studies in our group on bulk-film glass structural differences [20], that the glass network of the evaporated films are not identical to the parent glass. Hence, use of identical processing conditions are not expected to yield identical post-pressed surface behavior. For this reason development of pressing and post-press measurement techniques will continue with special attention paid to refine the time-force-temperature regime to precisely control the thermo-viscosity behavior of the glass in its appropriate film state. Additionally, we will elucidate how the geometry of the grooves can correlate, at constant stamping regime, to the resulting stamp feature uniformity. These results will be compared and evaluated using Computational Fluid Dynamic (CFD) methods being currently refined, with the process parameters being used as inputs for modeling of these efforts. Finally this refinement will involve the mapping of glass surface features with higher resolution methods, such as atomic force microscopy.

4. CONCLUSION

This study investigates the use of hard, hot-stamping of ChG bulk and thin films. We have demonstrated our ability to transfer features with sub-micron resolution onto As_2Se_3 glass bulk and thin films. Expertise and know-how will be extremely valuable to further optimize nanoimprint patterning of thermo-viscous ChGs for application where stable, complex, large-area features are targeted. Specifically it will allow addressing the efficiency limit and high fabrication cost of current light trapping methods by developing novel low-symmetry gratings for next-generation thin photovoltaic cells. Other complimentary efforts to this work [21] aim towards extension of these findings, towards the integration of stamped ChG structures to other photonic device structures on traditional and other, novel substrate platforms.

Acknowledgments
The authors acknowledge funding support provided by the US Department of Energy under award number DE-EE0005327. UCF co-authors also acknowledge funding provided in part by the US Department of Energy [Contract #DE- NA000421], NNSA/DNN R&D.

References
[1] Tekin, E., Smith, P. J. and Schubert U. S., "Inkjet printing as a deposition and patterning tool for polymers and inorganic particles," Soft Matter 4, 703–713 (2008).
[2] Zhao, X. M., Xia, Y. N. and Whitesides, G. M., "Soft lithographic methods for nano-fabrication," Jr. Mat. Chem. 7(7), 1069-1074 (1997).
[3] Campbell, C. J., Smoukov, S. K., Bishop, K., Baker, E. and Grzybowski, B. A., "Direct Printing of 3D and Curvilinear Micrometer-Sized Architectures into Solid Substrates with Sub-micrometer Resolution," Adv. Mater. 18(15), 2004–2008 (2006).
[4] Ofir, Y., Moran, I., Subramani, C., Carter, K. R. and Rotello, V. M., "Nanoimprint Lithography for Functional Three-Dimensional Patterns," Adv. Mater. 22(32), 3608–3614 (2010).
[5] Guo, L. J., "Nanoimprint Lithography: Methods and Material Requirements," Adv. Mater. 19, 495–513 (2007).
[6] Avnon, E., Yaacobi-Gross, N., Ploshnik, E., Shenhar, R. and Tessler, N., "Low cost, nanometer scale nanoimprinting – Application to organic solar cells optimization," Organic Electronics 12(7), 1241–1246 (2011).

[7] Zakery, A. and Elliott, S.R, "Optical properties and applications of chalcogenide glasses: a review," Jr. Non-Crystal. Solids 330, 1-12 (2003).
[8] Wuttig, M. and Yamada, N., "Phase-change materials for rewriteable data storage," Nature Mater. 6, 824-833 (2007).
[9] Eggleton, B., Luther-Davies, B. and Richardson, K., "Chalcogenide Photonics," Nature Photonics 5, 141-148 (2011).
[10] Song, S., Carlie, N., Boudies, J., Petit, L., Richardson, K. and Arnold, C. B., "Spin-coating of $Ge_{23}Sb_7S_{70}$ Chalcogenide Glass Thin Films", Jr. Non-Crystal. Solids 355, 2272-2278 (2009).
[11] Zou, Y., Lin, H., Ogbuu, O., Li, L., Danto, S., Novak, S., Wilkinson, J., Musgraves, J. D., Richardson, K. and Hu, J., "Effect of annealing conditions on the physio-chemical properties of spin-coated As_2Se_3 chalcogenide glass films," Opt. Mater. Express 2(12), 1723–1732 (2012).
[12] Hu, J., Carlie, N., Petit, L., Agarwal, A., Richardson, R. and Kimerling L., "Demonstration of chalcogenide glass racetrack microresonators" Opt. Express 33(8), 761-763 (2008).
[13] Madden, S. J., Choi, D. Y., Bulla, D. A., Rode, A. V., Luther-Davies, B., Ta'eed, V. G., Pelusi, M. D. and Eggleton, B. J., "Long, low loss etched As_2S_3 chalcogenide waveguides for all-optical signal regeneration," Opt. Express 15(22), 14414-14421 (2007).
[14] Semouchkina, E., Werner, D. H. Semouchkin, G. B. and Pantano, C., "An IR invisibility cloak composed of glass" Appl. Phys. Lett. 96, 233503-1/-3 (2010).
[15] Tsay, C., Mujagić, E., Madsen, C. K., Gmachl, C. F. and Arnold, C. B., "Mid-infrared characterization of solution-processed As_2S_3 chalcogenide glass waveguides," Opt. Express 18(15), 15523–15530 (2010).
[16] Silvennoinen, M., Paivasaari, K., Kaakkunen, J. J. J., Tikhomirov, V. K., Lehmuskero, A., Vahimaa, P. and Moshchalkov, V. V., "Imprinting the nanostructures on the high refractive index semiconductor glass," Applied Surface Science 257(15), 6829–6832 (2011).
[17] Han, T., Madden, S., Bulla, D. and Luther-Davies, B. "Low loss Chalcogenide glass waveguides by thermal nano-imprint lithography," Opt. Express 18(18), 19286-19291 (2010).
[18] Wachtel, P., Mosaddegh, P., Gleason, B., Musgraves, J. D. and Richardson, K., "Performance evaluation of a Bench-Top Precision Glass Molding Machine," Advances in Mechnical Engineering 2013, 178680 (2013).
[19] Musgraves, J. D., Wachtel, P., Novak, S., Wilkinson, J. and Richardson, K., "Composition dependence of the viscosity and other physical properties in the arsenic selenide glass system," Jr. Applied Physics 110, 063503 (2010).
[20] Schulte, A., Rivero, C., Richardson, K., Turcotte, K., Laniel, J., Hamel, V., Villeneuve, A., Saliminia, A. and Galstian, T., "Bulk-film structural differences of chalcogenide glasses probed in situ by near-infrared waveguide Raman spectroscopy" Opt. Communications 198, 125-128 (2001).
[21] Zou, Y., Zhang, D., Lin, H., Li, L., Morel, L., Zhou, J., Du, Q., Ogbuu, O., Danto, S., Musgraves, J. D., Richardson, K., Dobson, K., Birkmire, R. and Hu, J., "High-Performance, High-Index-Contrast Chalcogenide Glass Photonics on Silicon and Unconventional Nonplanar Substrates," Adv. Funct. Mater. *submitted* (2013)